LA-UR-11-10599
Approved for public release; distribution is unlimited.

Title: Quantitative Monitoring for Enhanced Geothermal Systems Using Double-Difference Waveform Inversion with Spatially-Variant Total-Variation Regularization

Author(s): Lin, Youzuo
Huang, Lianjie
Zhang, Zhigang

Intended for: GRC's 35th Annual Meeting, 2011-10-23/2011-10-26 (San Diego, California, United States)

Quantitative Monitoring for Enhanced Geothermal Systems Using Double-Difference Waveform Inversion with Spatially-Variant Total-Variation Regularization

Youzuo Lin, Lianjie Huang, and Zhigang Zhang
Los Alamos National Laboratory, Geophysics Group, MS D443, Los Alamos, NM 87545

Abstract

Double-difference waveform inversion is a promising tool for quantitative monitoring for enhanced geothermal systems (EGS). The method uses time-lapse seismic data to jointly inverts for reservoir changes. Due to the ill-posedness of waveform inversion, it is a great challenge to obtain reservoir changes accurately and efficiently, particularly when using time-lapse seismic reflection data. To improve reconstruction, we develop a spatially-variant total-variation regularization scheme into double-difference waveform inversion to improve the inversion accuracy and robustness. The new regularization scheme employs different regularization parameters in different regions of the model to obtain an optimal regularization in each area. We compare the results obtained using a spatially-variant parameter with those obtained using a constant regularization parameter. Utilizing a spatially-variant regularization scheme, the target monitoring regions are well reconstructed and the image noise is significantly reduced outside the monitoring regions. Our numerical examples demonstrate that the spatially-variant total-variation regularization scheme provides the flexibility to regularize local regions based on the *a priori* spatial information without increasing computational costs and the computer memory requirement.

1 Introduction

Quantitative monitoring for enhanced geothermal systems can help optimize the geothermal production and the placement of new wells. Conventionally, reservoir changes are obtained from differences of independent inversions of time-lapse data. Full-waveform inversion is a quantitative method for estimating subsurface geophysical properties. It can be implemented in both the time domain (Tarantola 1984; Mora 1987) and the frequency domain (Pratt et al. 1998; Sirgue and Pratt 2004). In recent years, many new full-waveform inversion schemes were developed based on regularization (Hu et al. 2009; Burstedde and Ghattas 2009; Ramirez and Lewis 2010), *a priori* information (Ma et al. 2010), preconditioning (Guitton and Ayeni 2010; Tang and Lee 2010), and dimensionality reduction (Moghaddam and Herrmann 2010). Images of the conventional approach for time-lapse seismic data usually contain significant noise and artifacts, and the values of changes in geophysical properties are not accurate. Watanabe et al. (2004) proposed a differential waveform tomography method in the frequency domain for time-lapse crosswell seismic data, and clearly showed its improvement compared to the conventional method. Denli and Huang (2009) introduced a double-difference elastic-waveform tomography method in the time domain for time-lapse surface seismic reflection data. These methods jointly invert time-lapse seismic data for reservoir changes.

To further improve the accuracy and robustness of double-difference waveform inversion, we develop a spatially-variant total-variation regularization scheme in combination with *a priori* spatial information. Regularization technique is often used in inverse problems (Vogel 2002; Tarantola 2005). The most often used regularization methods are L_2 norm based regularization (Tikhonov) and L_1 norm based regularization (total variation or compressive sensing). The spatially-variant regularization can improve inversion results for medical imaging, image restoration and other applications (Strong 1997; Guo and Huang 2009). We explore the use of the spatially-variant total-variation regularization scheme in double-difference full-waveform inversion. We solve the minimization of the misfit function using the block coordinate descent (BCD) scheme (Bertsekas 1999) in combination with the nonlinear conjugate gradient (NCG) approach (Nocedal and Wright 2000). The gradient of the misfit function is obtained using an adjoint method (Tarantola 1984; Tromp et al. 2005). We use a synthetic time-lapse seismic data for a Brady's EGS model to verify the advantages of the spatially-variant regularization scheme for double-difference waveform inversion. Our results demonstrate that the new method produces more accurate results of reservoir changes compared to those obtained using a constant regularization parameter.

2 Theory

2.1 Full-Waveform Inversion

The acoustic-wave equation in the time-domain is given by

$$\left[\frac{1}{K(\mathbf{r})}\frac{\partial^2}{\partial t^2} - \nabla\cdot\left(\frac{1}{\rho(\mathbf{r})}\,\nabla\right)\right] p(\mathbf{r},t) = s(t)\delta(\mathbf{r}-\mathbf{r}_0), \tag{1}$$

where $\rho(\mathbf{r})$ is the density, $K(\mathbf{r})$ is the bulk modulus, $s(t)$ is the source term, $\mathbf{r}_0$ is the source location, and $p(\mathbf{r},t)$ is the pressure field. The forward modeling using equation (1) can be written as

$$\mathbf{p} = f(\mathbf{K},\boldsymbol{\rho},\mathbf{s}), \tag{2}$$

where the function of f is a given nonlinear operator. Numerical techniques such as finite difference and spectral element methods can be used to solve (2). Let $\mathbf{m}$ be the model parameters, equation (2) becomes

$$\mathbf{p} = f(\mathbf{m}). \tag{3}$$

The inverse problem of equation (3) is usually posed as a minimization problem such that

$$E(\mathbf{m}) = \min_{\mathbf{m}} \left\{||\mathbf{d} - f(\mathbf{m})||_2^2\right\}, \tag{4}$$

where $E(\mathbf{m})$ is the misfit function, $||\cdot||_2$ stands the L_2 norm, and $\mathbf{d}$ represents recorded waveforms. The minimization of (4) is to find a model $\mathbf{m}$ that yields the minimum difference between observed and synthetic waveforms.

2.2 Double-Difference Waveform Inversion

Conventionally, two independent inversions in (4) are carried out to obtain the time-lapse changes in reservoir, that is

$$\delta\mathbf{m}_{\text{conv}} = f^{-1}(\mathbf{d}_{\text{time 2}}) - f^{-1}(\mathbf{d}_{\text{time 1}}), \tag{5}$$

where f^{-1} means the general inverse of waveform data, and $\mathbf{d}_{\text{time 1}}$ and $\mathbf{d}_{\text{time 2}}$ are data collected at two different times.

For double-difference waveform inversion, the data misfit in the cost function is replaced by

$$\delta d \equiv (\mathbf{d}_{\text{time 2}} - \mathbf{d}_{\text{time 1}}) - (\mathbf{d}_{\text{sim\_time 2}} - \mathbf{d}_{\text{sim\_time 1}}), \tag{6}$$

where the first term is the time-lapse difference in data, and the second term is the difference in synthetic time-lapse data. The method uses time-lapse seismic data to jointly invert for changes in reservoir geophysical properties.

3 *A Priori* Information and Spatially-Variant Regularization

3.1 The Roles of *A Priori* Information

A priori information plays an important role in the inverse problems. The usage of *a priori* information is usually to avoid the instability during the inversion of data (Tarantola 1984). It can be some reasonable initial guess of the solution, the smoothness of the desired reconstruction or the spatial information on the solution. In general, the *a priori* information is functioning as a guide to the true solution. More details on the effects of *a priori* information to inverse problem can be referred to (Hansen 1998; Vogel 2002; Tarantola 2005). In our work, we utilize both the spatial information and smoothness of the desired model as our *a prior* information.

There are different methods to incorporate the *a prior* information into inversion algorithms (Ma et al. 2010). We use regularization techniques in combination with the *a prior* information.

3.2 Total-Variation Regularization

Total-variation (TV) regularization is one regularization technique broadly used in image processing. The advantage of using TV is its edge-preserving capability. The misfit function for the TV scheme is

$$E(\mathbf{m}) = \min_{\mathbf{m}} \left\{ \|\mathbf{d} - f(\mathbf{m})\|_2^2 + \lambda \|\nabla \mathbf{m}\|_1 \right\} \text{ with } \lambda > 0, \tag{7}$$

where λ is the regularization parameter.

3.3 Spatially-Variant TV Regularization

Another equivalent form of the TV regularization in equation (7) is given as a constrained minimization problem, that is,

$$\begin{aligned} &\min_{\mathbf{m}} \left\{ \|\mathbf{d} - f(\mathbf{m})\|_2^2 \right\} \\ &\text{subject to } \|\nabla \mathbf{m}\|_1 \ \leq \ \epsilon, \end{aligned} \tag{8}$$

where the parameter ϵ plays the same role as λ in (7) to control the degree of regularization of the desired solution.

To incorporate the spatial information into (8), we modify (8) as

$$\begin{aligned} &\min_{\mathbf{m}} \left\{ \|\mathbf{d} - f(\mathbf{m})\|_2^2 \right\} \\ &\text{subject to } \|\nabla \mathbf{m}_i\|_1 \ \leq \ \epsilon_i, \ \mathbf{m}_i \in \Omega_i, \end{aligned} \tag{9}$$

where Ω_i is a spatial region, and ϵ_i is a spatially-variant parameter.

To incorporate the initial model, equation (9) is modified as

$$\begin{aligned} &\min_{\mathbf{m}} \left\{ \|\mathbf{d} - f(\mathbf{m})\|_2^2 \right\} \\ &\text{subject to } \|\nabla[\mathbf{m}_i - (\mathbf{m_0})_i]\|_1 \leq \epsilon_i,\ \mathbf{m}_i \in \Omega_i, \end{aligned} \tag{10}$$

where $\mathbf{m_0}$ is the initial model. The *a priori* information about the spatial characteristics of the model is used to determine spatial regions Ω_i.

3.4 Spatial *A Priori* Information

For the inverse problem based on equation (10), we need to know both the initial model $\mathbf{m_0}$ and spatial regions Ω_i. The starting model $\mathbf{m_0}$ may be obtained from ray tomography. Waveform inversion is the combination of migration and tomography (Mora 1989). Migration yields the shapes (or edges) of the anomalies and can be obtained in the first a few iterations during inversion. Therefore, these migration-like results can provide the information about the spatial regions Ω_i. For double-difference waveform inversion, the target monitoring regions are the *a priori* information to be used.

4 Numerical Algorithm and Implementation

4.1 Total-Variation Solver

Many numerical TV solvers have been proposed for solving (7) (Li and Santasa 1996; Vogel and Oman 1996, 1998; Wohlberg and Rodriguez 2007). We choose the one proposed in (Vogel and Oman 1998) because of its efficiency and simplicity. A small constant β is usually added to the TV term to enable the differentiability of the L_1 norm at the origin, i.e.

$$\mathrm{TV}(\mathbf{m}) = \|\nabla \mathbf{m}\|_1 \approx \sum_{i=1}^{n} \sqrt{(\mathrm{D}_i \mathbf{m})^2 + \beta^2}, \tag{11}$$

where $\mathrm{D}_i \mathbf{m} = \mathbf{m}_i - \mathbf{m}_{i-1}$. The gradient of the TV term can be further expressed using the divergence operator:

$$\nabla \mathrm{TV}(\mathbf{m}) = -\nabla \cdot \left(\frac{\nabla \mathbf{m}}{\sqrt{\mathbf{m} + \beta^2}} \right). \tag{12}$$

Therefore, a gradient-based line search algorithm can be performed once the gradient of the TV term is computed.

4.2 Optimization Algorithm for Spatially-Variant TV Regularization

Equation (10) is the object function for our spatially-variant TV regularization scheme. It can be solved by converting it into an equivalent non-constrained expression. Using the Lagrange multiplier (Nocedal and Wright 2000), we have

$$\begin{aligned} &E(\mathbf{m}) = \min_{\mathbf{m}} \left\{ \|\mathbf{d} - f(\mathbf{m})\|_2^2 + \sum_i \lambda_i \|\nabla[\mathbf{m}_i - (\mathbf{m_0})_i]\|_1 \right\}, \\ &\text{with } \lambda_i > 0, \text{ and } \mathbf{m}_i \in \Omega_i. \end{aligned} \tag{13}$$

The role of λ_i's is the same as ϵ_i's in (10) to regularize the reconstruction.

We employ a nonlinear conjugate gradient (NCG) line search approach (Nocedal and Wright 2000) to solve equation (13). The gradient of equation (13) varies for different spatial regions. We use the block coordinate descent (BCD) approach that has been proved to be efficient for such a situation (Bertsekas 1999; Wu and Lange 2008; Li and Osher 2009).

4.2.1 Block Coordinate Descent

Analogous to the Gauss-Seidel matrix solver algorithm in optimization, BCD partitions the coordinates into N blocks, and improves the estimation of the solution in each block by minimizing along one direction with all the other blocks fixed. The order in which the blocks are visited is called "sweep pattern." The order of the blocks visited does matter in BCD algorithm. In our algorithm, we use a "cyclic pattern," which means all the blocks are visited sequentially. It has been illustrated that using different visiting orders may help in improving the convergence rate of the algorithms (Wu and Lange 2008; Li and Osher 2009).

To ensure the convergence as in the line search algorithm, the search direction $\mathbf{d}_k$ along each block needs to be a descent direction. In the other words, for the function $E(\mathbf{m})$, $\mathbf{d}_k$ needs to satisfy

$$cos\,\theta = \frac{\nabla E_k^T \boldsymbol{\gamma}_k}{\|\nabla E_k\|\ \|\boldsymbol{\gamma}_k\|} < 0, \tag{14}$$

where θ is the angle between the search direction and ∇E_k. We use the conjugate-gradient direction as the search direction for each block.

After obtaining the search direction for a particular block, the line search with the Armijo criteria is further utilized for the optimal step size. We then update the block with the search direction and its step size without affecting other blocks:

$$\mathbf{m}_i^{k+1} = \mathbf{m}_i^k + \alpha_i^k \boldsymbol{\gamma}_i^k, \tag{15}$$

where the superscripts stands for the iteration number and the subscript stands for the block index.

4.2.2 Nonlinear Conjugate Gradient

The search directions in BCD are calculated from nonlinear conjugate gradients, as illustrated in Nocedal and Wright (2000). The method to incorporate BCD with NCG is to replace the updating step (step 3) in Algorithm 1 with (15).

5 Numerical Results

We use synthetic time-lapse surface seismic data for the models in Fig. 1 to demonstrate the improvement of the double-difference waveform inversion with a spatially-variant TV regularization scheme. The models are constructed using geologic features found at the Brady's EGS site. They contain several steep fault zones. There is a region in Fig. 1b with a decreased velocity due to water/fluid injection for stimulation, as shown in Fig. 1c. Twenty common-shot gathers of synthetic time-lapse seismic data with 500 receivers at the top of the models are used to jointly invert for the reservoir change. The shot interval is 125 m and the receiver interval is 5 m. A Ricker's wavelet with a center frequency 25 Hz is used as the source function.

Algorithm 1 Canonical NCG to solve $\min_{\mathbf{m}} E(\mathbf{m})$

Input: $\mathbf{m}^0$, TOL
Output: $\mathbf{m}^k$

Initialize $k = 0$, $E^0 = E(\mathbf{m}^0)$, $\nabla E^0 = \nabla E(\mathbf{m}^0)$;
while $||\nabla E^k|| > \text{TOL}$ **do**
  Compute α^k and update the solution $\mathbf{m}^{k+1} = \mathbf{m}^k + \alpha^k \boldsymbol{\gamma}^k$;
  Evaluate ∇E^{k+1};
  $\beta^{k+1} = \frac{<\nabla E^{k+1}, \nabla E^{k+1}>}{<\nabla E^k, \nabla E^k>}$;
  $\boldsymbol{\gamma}^{k+1} = -\nabla E^{k+1} + \beta^{k+1} \boldsymbol{\gamma}^k$;
  $k \longleftarrow k + 1$;
end while

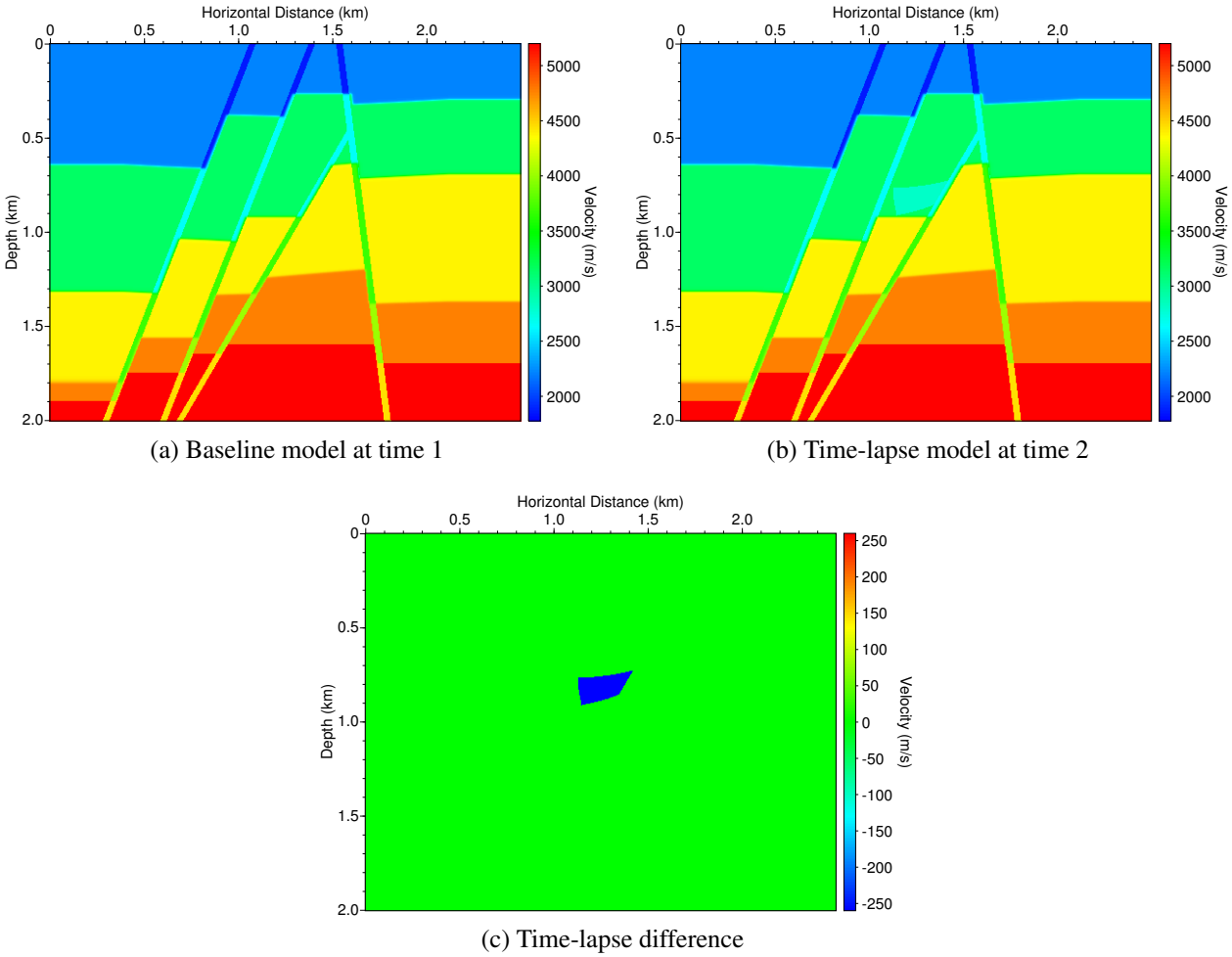

(a) Baseline model at time 1

(b) Time-lapse model at time 2

(c) Time-lapse difference

Figure 1: The baseline velocity model (a) and the time-lapse velocity model (b) that contains a region with a decreased velocity shown in (c) due to fluid injection for stimulation. The models contain several steep fault zones. They are constructed using geologic features found at Brady's EGS site.

Fig. 2 demonstrates the improvement of waveform inversion using the TV regularization for the baseline model. The figure shows the differences between the reconstructed models and the starting model, and the true difference between the starting model and the baseline model. The result with

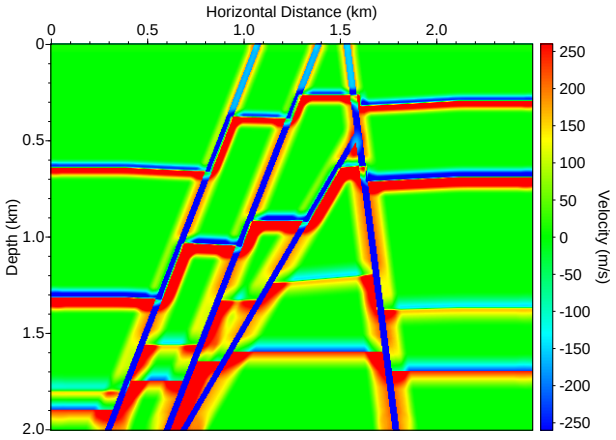

(a) True baseline difference

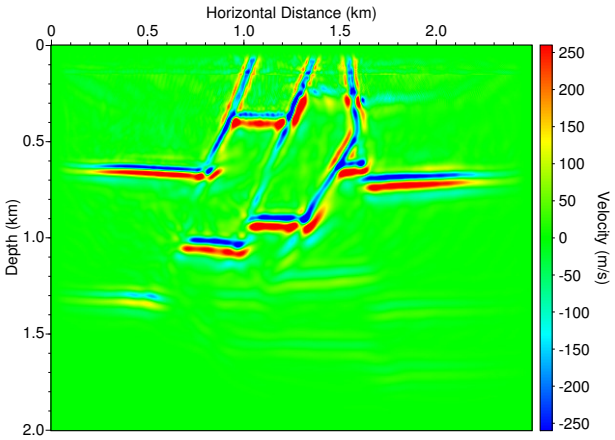

(b) Reconstruction of the difference without regularization

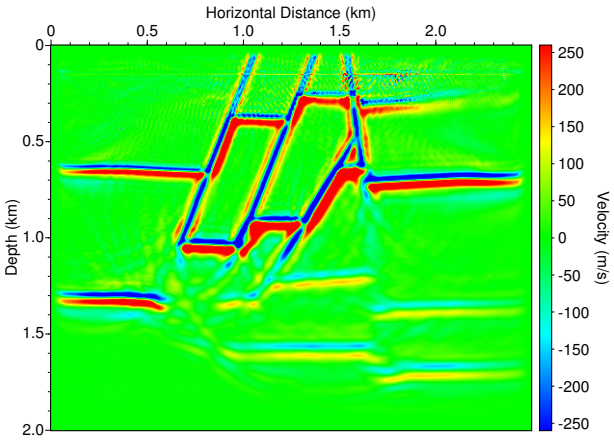

(c) Reconstruction of the difference with TV

Figure 2: (a) The difference between the starting model for waveform inversion and the true baseline model. (b) The difference between the reconstructed model obtained without any regularization and the starting model. (c) The difference between the reconstructed model obtained with TV regularization and the starting model. The result in (c) is clearly better than that in (b), particularly in the deep region of the model.

the TV regularization in Fig. 2c shows the better reconstruction in the entire model, particularly in the deep region of the model that cannot be reconstructed without using any regularization.

For comparison, we first obtain the velocity change in the target monitoring region using the conventional approach by subtracting the two independent inversions and using the double-difference waveform inversion with a constant regularization parameter. The result of the conventional approach in Fig. 3 contains significant image artifacts. The vertical profile in Fig. 3b shows that the reconstructed velocity change in the target region is approximately -200 m/s, significant different from the true value of -320 m/s. In addition, it contains significant image noise above and below the target monitoring region.

Figure 4 shows the result of double-difference waveform inversion with a constant regularization parameter $\lambda = 1.0 \times 10^{-13}$. The reconstructed velocity change in the target region is approximately -260 m/s, which is closer to the true value of -320 m/s compared to that obtained using the conventional approach (Fig. 3b). Figure 4 contains fewer noise than Fig. 3.

In order to incorporate the *a priori* spatial information into the spatially-variant TV regularization scheme for double-difference waveform inversion, we determine the target monitoring re-

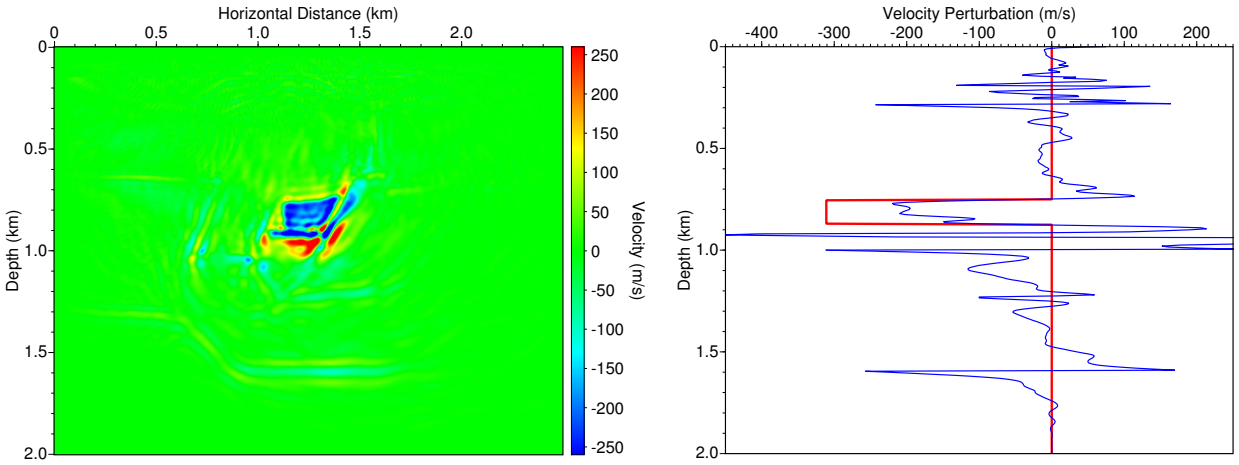

(a) The difference of two independent inversions

(b) A vertical profile of the result in (a)

Figure 3: The difference (a) of two independent inversions of synthetic time-lapse seismic data for the models in Fig. 1 together with a vertical profile (b) at the horizontal position of 1250 m of the result in (a). The red line in (b) shows the true velocity change, and the blue line is the difference of two independent inversions.

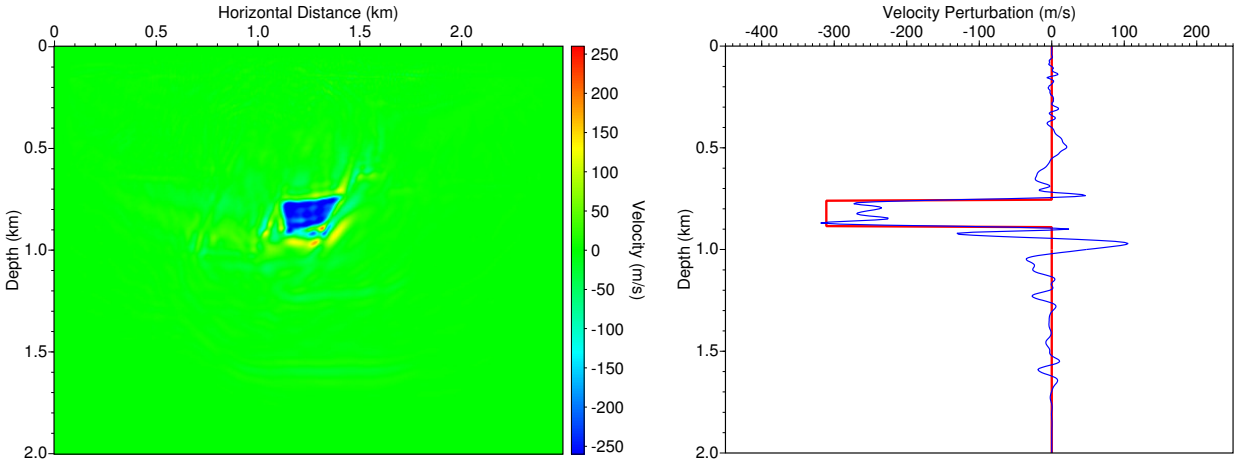

(a) Reconstructed velocity difference

(b) A vertical profile of the result in (a)

Figure 4: The result of double-difference waveform inversion with a constant regularization parameter $\lambda = 1.0 \times 10^{-13}$ together with a vertical profile at the horizontal position of 1250 m. The red line in (b) shows the true velocity change, and the blue line is the result of double-difference waveform inversion with a constant regularization parameter.

gions using the result of the first a few iterations. There are two regions in equation (13) for our time-lapse models in Fig.1, one within the target monitoring region, and the other outside the target monitoring region. The regularization parameter utilized for the target monitoring region is $\lambda_{in} = 1.0 \times 10^{-13}$, and $\lambda_{out} = 1.0 \times 10^{-10}$ for the other region. Figure 5 shows the result of double-difference waveform inversion with a spatially-variant regularization parameter. The reconstructed velocity change in the target monitoring region is close to the true value of -320 m/s. Figure 5 contains significant fewer image artifacts outside the target monitoring region compared to Fig. 3 and Fig. 4.

The computational cost of the double-difference waveform inversion with a spatially-variant TV regularization parameter is comparable to that with a constant regularization parameter.

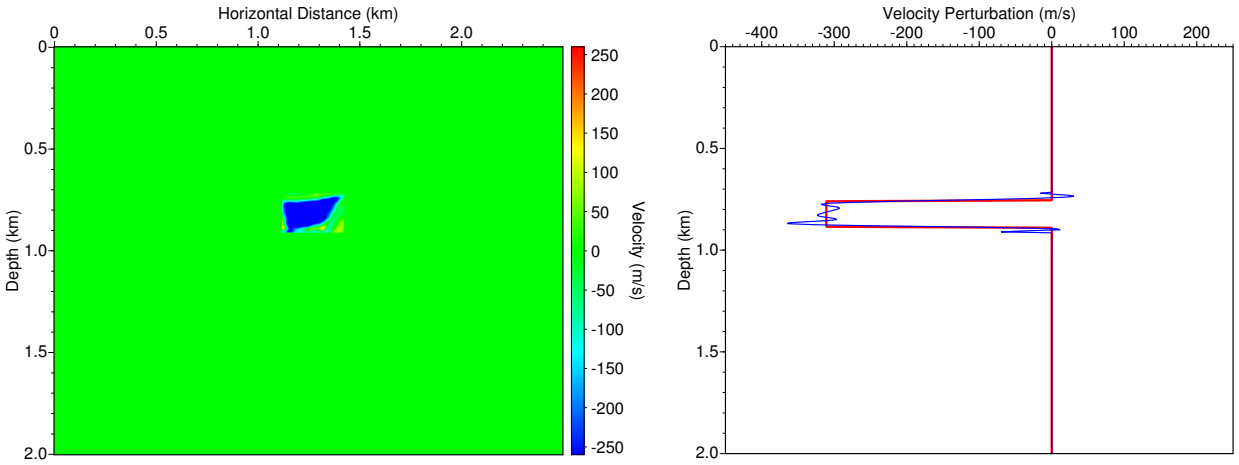

(a) Reconstructed velocity difference

(b) A vertical profile of the result in (a)

Figure 5: The result of double-difference waveform inversion with a spatially-variant regularization parameter together with a vertical profile at the horizontal position of 1250 m. The red line in (b) shows the true velocity change, and the blue line is the result of double-difference waveform inversion with spatially-variant TV regularization.

6 Conclusions

We have developed a spatially-variant TV regularization scheme for double-difference waveform inversion. The method employs different regularization parameters in different regions in space in combination with the spatial *a priori* information, or the target monitoring regions. It uses the block coordinate descent and nonlinear conjugate gradient schemes to solve the minimization problem. Our results of synthetic time-lapse seismic data for the Brady's EGS models demonstrate that our new method can reconstruct accurate values of velocity changes due to water/fluid injection for stimulation. The new method can produce images of reservoir changes with much fewer image artifacts than those obtained using double-difference waveform inversion with a constant regularization parameter. The double-difference waveform inversion with the spatially-variant total-variation regularization can quantify the spatial and temporal changes in reservoirs of enhanced geothermal systems using time-lapse seismic data. It is a useful tool for optimizing the production of enhanced geothermal systems.

Acknowledgements

This work was supported by the Geothermal Technologies Program of the U.S. Department of Energy through contract DE-AC52-06NA25396 to Los Alamos National Laboratory. We thank Dr. John Queen of Hi-Q Geophysical Inc. for providing us with a velocity model of the Brady's EGS field.

References

Bertsekas, D. P., 1999, Nonlinear programming: Athena Scientific.

Burstedde, C., and O. Ghattas, 2009, Algorithmic strategies for full waveform inversion: 1d experiments: Geophysics, **74**, 37–46.

Denli, H., and L. Huang, 2009, Double-difference elastic waveform tomography in the time domain: 79th Annual International Meeting, SEG, Expanded Abstracts, 2302–2306.

Guitton, A., and G. Ayeni, 2010, A preconditioning scheme for full waveform inversion: 80th Annual International Meeting, SEG, Expanded Abstracts, 1008–1012.

Guo, W., and F. Huang, 2009, Adaptive total variation based filtering for MRI images with spatially inhomogeneous noise and artifacts: ISBI, 101–104.

Hansen, P. C., 1998, Rank-deficient and discrete ill-posed problems: Numerical aspects of linear inversion: SIAM.

Hu, W., A. Abubakar, and T. Habashy, 2009, Simultaneous multifrequency inversion of full-waveform seismic data: Geophysics, **74**, 1–14.

Li, Y., and S. Osher, 2009, Coordinate descent optimization for l_1 minimization with application to compressed sensing: a greedy algorithm: Inverse Problem Imaging, **3**, 487–503.

Li, Y., and F. Santasa, 1996, A computational algorithm for minimizing total variation in image restoration: IEEE Transaction on Image Processing, **5**, 987–995.

Ma, Y., D. Hale, Z. Meng, and B. Gong, 2010, Full waveform inversion with image-guided gradient: 80th Annual International Meeting, SEG, Expanded Abstracts, 1003–1007.

Moghaddam, P., and F. J. Herrmann, 2010, Randomized full-waveform inversion: a dimensionality-reduction approach: 80th Annual International Meeting, SEG, Expanded Abstracts, 977–982.

Mora, P., 1987, Nonlinear two-dimensional elastic inversion of multioffset seismic data: Geophysics, **54**, 1211–1228.

———, 1989, Inversion = migration + tomography: Geophysics, **54**, 1575–1586.

Nocedal, J., and S. Wright, 2000, Numerical optimization: Springer.

Pratt, R. G., C. Shin, and G. J. Hicks, 1998, Gauss-newton and full newton methods in frequency-space seismic waveform inversion: Geophysical Journal International, **13**, 341–362.

Ramirez, A., and W. Lewis, 2010, Regularization and full-waveform inversion: A two-step approach: 80th Annual International Meeting, SEG, Expanded Abstracts, 2773–2778.

Sirgue, L., and R. G. Pratt, 2004, Efficient waveform inversion and imaging: A strategy for selecting temporal frequency: Geophysics, **69**, 231–248.

Strong, D., 1997, Adaptive total variation minimizing image restoration: PhD thesis, University of California at Los Angeles.

Tang, Y., and S. Lee, 2010, Preconditioning full waveform inversion with phase-encoded hessian: 80th Annual International Meeting, SEG, Expanded Abstracts, 1034–1038.

Tarantola, A., 1984, Inversion of seismic reflection data in the acoustic approximation: Geophysics, **49**, 1259–1266.

———, 2005, Inverse problem theory: SIAM.

Tromp, J., C. Tape, and Q. Liu, 2005, Seismic tomography, adjoint methods, time reversal and banana-doughnut kernels: Geophysical Journal International, **160**, 195–216.

Vogel, C., 2002, Computational methods for inverse problems: SIAM.

Vogel, C. R., and M. E. Oman, 1996, Iterative methods for total variation denoising: SIAM Journal on Scientific Computing, **17**, 227–238.

———, 1998, A fast, robust algorithm for total variation based reconstruction of noisy, blurred imagesc: IEEE Transaction on Image Processing, **7**, 813–824.

Watanabe, T., S. Shimizu, E. Asakawa, and T. Matsuoka, 2004, Differential waveform tomography for time-lapse crosswell seismic data with application to gas hydrate production monitoring: 74th Annual International Meeting, SEG, Expanded Abstracts, 2323–2326.

Wohlberg, B., and P. Rodriguez, 2007, An iteratively reweighted norm algorithm for minimization of total variation functionals: IEEE Transaction on Image Processing, **14**, 948–951.

Wu, T., and K. Lange, 2008, Coordinate descent algorithm for lasso penalized regression: The Annals of Applied Statistics, **2**, 224–244.